

Optical properties of Sc films in the far and the extreme ultraviolet

Authors: Juan I. Larruquert^a, José A. Aznárez^a, José A. Méndez^a, Andrea Marco Malvezzi^b, Luca Poletto^c, Sara Covini^b

Affiliation: ^a Instituto de Física Aplicada-Consejo Superior de Investigaciones Científicas, C/ Serrano 144, 28006 Madrid, Spain

Phone: 34 91 561 8806; Fax: 34 91 411 7651

Email: larruquert@io.cfmac.csic.es

^b Dipartimento di Elettronica, Università di Pavia and INFM, Via Ferrata, 1, I27100 Pavia, Italy

^c Dep. of Information Engineering (Padova), Laboratory for UV and X-Ray Optical Research - INFM

Abstract

The optical properties of thin Sc films deposited in ultra high vacuum conditions have been investigated in the 6.7-174.4 nm spectral range. Transmittance and multi-angle reflectance were measured in situ in the 53.6-174.4 nm spectral range and they were used to obtain the complex refractive index of Sc films at every individual wavelength investigated. Transmittance measurements were made on Sc samples that were deposited over grids coated with a support C film. The transmittance and the extinction coefficient of Sc films at wavelengths shorter than 30 nm were measured ex situ. The ex situ samples were protected with an additional top C film before removal from vacuum. To our knowledge, these are the first optical measurements on Sc films reported in the present spectral range.

OCIS codes: 260.7200 Ultraviolet, extreme; 260.7210 Ultraviolet, far; 120.4530

Optical constants; 350.2450 Filters, absorption; 310.6860 Thin films: optical properties

1. INTRODUCTION

The optical constants (i.e., the real and imaginary parts of the refractive index) of many materials have not yet been measured in several regions of the extreme ultraviolet (EUV), which refers here to wavelengths shorter than 200 nm. This is the case for most materials of the lanthanide group, because their high reactivity versus residual gases, even in UHV, adds to the general difficulty in performing optical measurements in the EUV range. Sc and Y are often considered as members of the lanthanide group due to their similar chemical properties. This paper addresses the optical properties of Sc films. Scarce literature is available on the optical properties of Sc in the EUV. Optical measurements on any kind of Sc samples have been restricted to wavelengths longer than 225.4 nm: Weaver and Olson¹ measured absorptivity on single Sc crystals in the 248.0-6200 nm range, and Sigrist et al.² measured near normal reflectivity of Sc films in the 225.4-5635 nm. They also investigated reflectivity at shorter wavelengths, but only for Sc samples exposed to the air, which were most probably oxidized. Other than optical measurements, electron energy-loss (EEL) measurements have been performed on Sc samples by Brousseau-Lahaye et al.³, Cukier et al.⁴, and Onsgaard et al.⁵. Refs. 3 and 4 used the EEL measurements to obtain the loss function $-\text{Im}(1/\varepsilon)$, where ε is the dielectric constant; ε equals the square of the complex refractive index of the material. Brousseau-Lahaye et al. also calculated the complex dielectric constant of Sc films in the ~22.5-200 nm range by applying the Kramers-Kronig (KK) analysis to the loss function data. Sample preparation and handling is not clear either in Brousseau-Lahaye's or in Cukier et al.'s papers, but to the best of our understanding their samples were exposed to atmosphere and they were probably placed in contact with unspecified solvents. The reactivity of Sc may have resulted in hydride and/or oxide formation, apart from other possible contamination.

Sc films have been proposed and used as a component for multilayer coatings designed for the largest possible reflectance at wavelengths slightly longer than the Sc M edge (~36 nm) and L edge (3.2 nm). Theoretical calculations of the optical constants of Sc in the EUV have been performed by Uspenskii et al.⁶, but they provided no experimental data. For some materials other than Sc also investigated in Ref. 6 for which experimental data are available, the agreement with the theoretical calculations is poor. The authors of this paper used those calculations in the design of Sc/Si multilayer that were optimized for a large reflectance at individual wavelengths in the 35-50 nm spectral range^{7,8}, and in fact they fabricated multilayers with a remarkably high reflectance. However, there was a large difference between theoretical and experimental data, which may be due in part to optical constant inaccuracies.

The present paper addresses the lack of information on optical constants of Sc in the EUV. The experimental techniques used are described in Section 2. Section 3 reports the experimental data. The transmittance and reflectance measurements in the long EUV ($\lambda \geq 53.6$ nm) were performed on freshly prepared Sc films. We also performed transmittance measurements in the short EUV ($\lambda < 30$ nm) on ex situ Sc films that had been protected with a C film before extracted from vacuum. The optical constants n , k and the loss function were derived in the 53.6-174.4 nm range; k was obtained in several wavelengths and bands in the 6.7-30 nm range. The effect of sample aging under vacuum was also investigated.

2. EXPERIMENTAL TECHNIQUES

Sample deposition and optical measurements in the 53.6-174.4 nm range were performed in a reflectometer equipped for in situ ultra high vacuum (UHV) thin film deposition at the Instituto de Física Aplicada-CSIC, Madrid. The reflectometer-deposition system has been described elsewhere^{9,10}. The system basically consists of two interconnected UHV chambers: one for thin film deposition and the other for reflectance measurements. Each chamber is pumped with an ion pump and a titanium sublimation pump. The reflectometer chamber was baked out at 470 K. Sc lumps of 99.999% purity supplied by Stanford Materials were sublimated using W baskets and boats. Sc films were deposited onto room-temperature substrates. The average deposition rate ranged between 0.03 and 0.1 nm/s, with instantaneous rate peaks up to ~2 nm/s. These peaks were due to the fast evaporation of a certain small Sc particle whose temperature would suddenly rise due to an enhanced thermal contact with the boat or basket. The thickness of Sc films was monitored with a quartz crystal oscillator, which was calibrated through Tolansky interferometry.

Reflectance and transmittance measurements were performed in situ in the spectral region 53.6 – 174.4 nm. The base pressure in the deposition chamber and in the reflectometer (when isolated from the lamp-monochromator) were $\sim 4 \times 10^{-7}$ and $\sim 3 \times 10^{-8}$ Pa, respectively. The pressure in the deposition chamber increased during Sc deposition up to $\sim 1 \times 10^{-6}$ - 1×10^{-5} Pa. After the deposition of Sc, the pressure in the chamber decreased down to ~ 1 - 4×10^{-7} Pa, which was attributed to gettering properties of Sc for H₂. Within about 3 minutes from deposition the Sc sample was transferred in vacuum to the reflectometer chamber for reflectance or transmittance measurements in the 53.6-174.4 nm range. The total pressure in the reflectometer during reflectance/ transmittance

measurements, i.e. when the reflectometer is connected to the lamp-monochromator through a series of differential pumping devices, was $\sim 1.5 \times 10^{-7}$ Pa. The main component of the residual atmosphere in the reflectometer during reflectance/transmittance measurements was the non-oxidizing gas mixture continuously flowing in the discharge lamp. A small fraction of this flow reached the UHV reflectometer chamber through the multiple differential pumping arrangement. The gas mixture composition was: 93% He, 3% Ne, 3% Ar, and 1% N₂.

Two different kinds of substrates, one for reflectance and another one for transmittance measurements, were used. Reflectance measurements were performed on Sc films deposited over 50.8x50.8x3-mm³ float glass substrates that had been additionally polished by the manufacturer. Transmittance measurements were performed in the 53.6-104.8 nm range in situ by depositing Sc over a nickel grid previously coated with a C film. The grids had square holes with the following nominal characteristics: 5- μ m bar, 7.6- μ m hole (that corresponds to mesh 2000), 36% open area. The grids were first coated with a collodion film on which a thin C film was later deposited either by arc-evaporation or with an electron beam. The collodion film was then dissolved and only the C film remained over the grid. The procedure was performed according to well-known transmission electron microscopy techniques¹¹. C film thickness was of the order of 10 nm.

Transmittance measurements in the 6.7-30 nm range were performed ex situ. Sets with several grids were first coated with support C films according to the procedure described in the previous paragraph. C deposition was performed in a single run to guarantee constant C thickness through the set. Sc films of different thicknesses were

deposited sequentially over each of the C coated grids of a set. To avoid contamination of Sc films during the storage period necessary for sample transport to the reflectometers for measurements in the 6.7-30 nm range, the samples were overcoated with a protective C film before extracting them from vacuum. The protective top C film was deposited in situ by electron beam evaporation, which was performed simultaneously over all the samples of the set. The Sc samples were then C-Sc-C sandwiches on a nickel grid support. The samples within a set only differed in the Sc film thickness, and the effect of the grid and of the two C films results in a constant reduction factor of the sample transmittance. Each of the two protective C films had thicknesses in the 10-20 nm range. The variation of the C thickness throughout a set of samples is within a 5% of the average.

Each set of samples was removed from vacuum and quickly placed along with dessicant in plastic bags under dry N₂. The samples were transported to the reflectometers of LUXOR Laboratory (Padova) or of University of Pavia for short-wavelength transmittance measurements. The samples were stored under vacuum and the total period of time that they were out of vacuum before characterization was ~24-36 hours.

Transmittance measurements in Pavia were carried out with a calibration facility¹² based on a grazing incidence monochromator¹³ and a soft X-ray source. The former is equipped with a 600 lines/mm, 2-m radius, spherical grating working at an angle of incidence of 88° or 86°. The EUV radiation is emitted by a microfocus soft X-ray source with interchangeable anodes. An electron beam emitted by a tungsten filament (i.e. the cathode) is accelerated and focused on a target anode, stimulating the emission of radiation from core shell energy levels of the target. The source was used with Al and

Mg anodes emitting L-band radiation¹⁴. The source was coupled to the monochromator through a spherical gold mirror at 10° grazing angle in order to a) improve radiation throughput and b) reject undesired high energy radiation. Remotely controlled actuators allow translation of the samples across the monochromatic beam emerging from the exit slit. The intensity of the incident and transmitted radiation is monitored by a channel electron multiplier detector working in the photon counting mode. A data collection system (counter plus PC) automatically collects data and operates the apparatus. The emission bands of Al and Mg were used as a broadband source and individual wavelengths could be selected and scanned within the bands.

The transmittance measurements in the 6.7-13.5 nm spectral region using several anodes were performed in the soft X-ray test facility available in the LUXOR Laboratory in Padova¹⁵. The EUV radiation is emitted by a microfocus soft X-ray source with interchangeable anodes, the same model used in Pavia. The lines used to perform the measurements are K B (6.7 nm), M Y (9.2 nm), K Be (11.4 nm) and L Si (13.5 nm). Since no fine spectroscopic structures are expected from Sc in this spectral region, the whole emission bands of B, Y, Be and Si were used as a radiation source and no scanning through the bands was performed. The facility consists of a grazing incidence monochromator with a 1200 lines/mm spherical grating, an exit slit, and a toroidal mirror that focuses the beam onto the sample under test. The latter can be moved independently in the three spatial coordinates in order to control the illuminated area, and it can be extracted from the beam direction in order to measure the direct beam. A channel electron multiplier detector working in photon counting mode detects the direct beam or the beam transmitted through the sample.

All measurements were performed over samples placed at room temperature.

3. EXPERIMENTAL RESULTS

Fig. 1 shows the transmittance measured for Sc films of different thicknesses. For in situ measurements (53.6-104.8 nm), Fig. 1 represents the transmittance ratio of a film plus substrate to that of the uncoated substrate in order to separate the absorption of Sc from that of the C-grid substrate. For ex situ measurements ($\lambda < 30$ nm), the transmittance of a C-Sc-C-grid sample is normalized to the transmittance of a reference C-C-grid sample prepared in the same set. The lines in this and other figures are drawn to help the eye. In the 53.6-104.8 nm spectral range the transmittance of Sc increases when decreasing wavelength and we expect that transmittance remains increasing towards wavelengths shorter than 53.6 nm. Unfortunately there are gaps between the ranges covered. A minimum in transmission was measured at ~ 27 nm.

The semi-empirical approach of Henke et al.¹⁶ allows calculation of approximate values of transmittance of materials based on the assumption that condensed matter may be modeled as a collection of non-interacting atoms. This assumption is generally acceptable for wavelengths sufficiently far from absorption thresholds, and in any case smaller than ~ 41 nm¹⁷. Outside the validity domain, the specific chemical state is fundamental and direct experimental measurements must be performed. The transmittance of Sc calculated with the Henke approach using the web page of the Center for X-Ray Optics (CXRO) at Lawrence Berkeley National Laboratory¹⁸ shows an absorption peak centered at ~ 32.7 nm, and a band of low absorption longward of this wavelength. Our experimental measurements show a shift in the absorption peak compared to calculations with the Henke model.

By analogy with data obtained with Henke model, it is plausible to expect that Sc has a low absorption band starting at 27 nm and connecting the spectral region measured on ex situ samples with the transmittance measurements performed on in situ samples above 53.6 nm. If this were true, Sc films would be a potential candidate for EUV filters. The transmission band of Sc lies close to transmission bands of a few other materials, such as Al, Sb, Be, Bi, Ge, Si, Ti, Yb¹⁹, etc., some of which have been used as EUV filters. The peak position and bandwidth of Sc is different from those of the other materials. This may give an opportunity to Sc either as a single-material filter or in combination with one or more of the above materials if a narrower bandwidth is desired. The low absorption of Sc in this band makes it suitable also for multilayers, and Sc has already been used for this purpose in combination with Si^{7, 8}.

Reflectance measurements as a function of the incidence angle were performed in situ over freshly deposited Sc samples in the 53.6-174.4 nm spectral range. Fig. 2 shows the reflectance as a function of wavelength for the measured incidence angles. The reflectance measurements were performed in the horizontal plane of incidence of the reflectometer. Sigrist et al.² found that the reflectance of Sc at wavelengths longer than 225 nm decreases when Sc is exposed to the atmosphere. Tests on Sc films will show below that the reflectance in the EUV is also reduced upon short exposure to air at low pressure.

The transmittance as a function of thickness was used to obtain the Sc extinction coefficient k , which is the imaginary part of the refractive index ($N=n+ik$; i : imaginary unit), by using:

$$\frac{T_{fs}}{T_s} = \exp\left(-\frac{4\pi kx}{\lambda}\right) \quad (1)$$

where T_s and T_{fs} represent the transmittance of the uncoated substrate and of the substrate coated with a Sc film, respectively, (in situ measurements) or the transmittance of the reference C-C sample and of a C-Sc-C sandwich of the same sample set, respectively (ex situ measurements). x stands for the Sc film thickness. For the 53.6-104.8 nm spectral range Sc samples were prepared in which a new Sc film was deposited over a first Sc film and this process was repeated several times. The transmittance was measured for the uncoated substrate and after every Sc deposition without breaking vacuum. A log plot of the transmittance versus thickness is shown in Fig. 3. The transmittance of sets of samples prepared in the same run are also plotted for some wavelengths below 30 nm. k values obtained from transmittance measurements are displayed in Fig. 4a (Fig. 4b) as a function of wavelength above 50 nm (below 30 nm).

The reflectance measurements in the 53.6-174.4 nm spectral range were used to calculate the optical constants of Sc. In the 53.6-104.8 nm sub-range, the real part of the refractive index of Sc films was obtained from the reflectance measurements, once the imaginary part (extinction coefficient) had been obtained from transmittance measurements. In the 106.7-174.4 nm sub-range, in which the high absorption of Sc turned transmittance measurements in a difficult task, both n and k were calculated by fitting the multi-angle reflectance measurements.

When the film is not completely opaque to radiation, the film/ substrate interface gives a contribution to reflectance. In the optical constant calculation of Sc from reflectance measurements we took into account the interface thin film/ glass substrate. In the calculation we used optical constants of glass substrates previously obtained. The amplitude reflectance of the vacuum/ thin film/ glass substrate multilayer is given by:

$$r^{s,p} = \frac{r_{01}^{s,p} + r_{12}^{s,p} \exp(2i\beta)}{1 + r_{01}^{s,p} r_{12}^{s,p} \exp(2i\beta)} \quad (2)$$

where $r_{ij}^{s,p}$ are the Fresnel reflection coefficients at the interface ij for both parallel (p) or perpendicular (s) electric vector. 0 stands for vacuum, 1 for the thin film, and 2 for the substrate. The propagation function β is given by:

$$\beta = k_0 x (N_1^2 - N_0^2 \sin^2 \theta)^{1/2} \quad (3)$$

where θ is the angle of incidence of the incident beam, x is the film thickness, N_0 is the refractive index of vacuum ($N_0=1$), N_1 is the complex refractive index of the thin film, and k_0 is the free space wavevector.

Radiation emerging from the monochromator onto the sample is partially polarized. The influence of polarization on reflectance can be described through a single parameter that will be referred to as the degree of polarization p :

$$p = \frac{I_p - I_s}{I_p + I_s} \quad (4)$$

where I_p and I_s indicate the fraction of the incident intensity with the electric vector parallel and perpendicular, respectively, to the plane of incidence. With this notation, the reflectance (ratio of reflected to incident radiation intensity) of the vacuum/ thin film/substrate multilayer for a certain degree of polarization is given by:

$$R = \frac{1+p}{2} R_p + \frac{1-p}{2} R_s \quad (5)$$

where R_p and R_s are the intensity reflectance for p and s polarization, i.e. they equal the square modulus of the amplitude reflectance for parallel and perpendicular incidence, respectively, as they are given in Eq. 2.

The search for the refractive index of films was made by the minimization of the following merit function:

$$s^2 = \sum_{i=1, \dots, m} \left\{ R^{\text{exp}}_{\theta(i)} - R[\theta(i), n, k, p] \right\}^2 \quad (6)$$

where $R^{\text{exp}}_{\theta(i)}$ is the reflectance measured at the angle of incidence $\theta(i)$, and $R[\theta(i), n, k, p]$ is the calculated reflectance for the trial value of the real part of the refractive index n , using k values obtained from transmittance measurements as known parameters (53.6-104.8 nm spectral range) or for the trial values of n and k (106.7-174.4 nm spectral range). p for each wavelength in our monochromator had been previously determined. The number of angles of incidence was $m=9$, namely 5° , 15° , 25° , 35° , 45° , 55° , 65° , 75° , and 80° , all of them in the horizontal plane of incidence of the reflectometer. Regarding surface roughness, a 0.6-nm RMS roughness was measured for the glass substrate by means of atomic force microscopy. We assumed that the surface roughness after

depositing Sc was not appreciably larger than for the bare substrate. The surface roughness was neglected in the calculation. The optical constants n and k of Sc, calculated with the above model, are plotted in Fig. 4a. The optical constants of Sc are also shown in Table 1.

We here discuss about the optical constants obtained above. Calculations performed with the Henke model are displayed in Fig 4b. The only experimental optical constants available so far were those from Brousseau-Lahaye et al.³, which were obtained from EEL measurements using the KK analysis. We calculated n and k from Ref. 3's dielectric constant and we plotted them both in Figs. 4a and 4b. The extinction coefficient obtained with the emission bands of B, Y, Be, Si, and Al anodes is in good agreement with the Henke model. Measurements performed within the emission band of Mg match Henke's data below ~ 28 nm, but the two figures suddenly disagree, as if the onset of Sc were at a wavelength shorter than the prediction. As expressed above, the Henke model is not accurate close to the absorption edges. Above 35 nm Brousseau-Lahaye's extinction coefficient data decreases slightly, and it does not show a clear transmission band; at 53.6 nm k is a factor of ten larger than our results on in situ samples. The different behavior obtained by Brousseau-Lahaye et al. with respect to our in situ measurements can be attributed to contamination of their samples, which were apparently exposed to atmosphere, and/or to the approximations they used to obtain the dielectric constant.

Summarizing, the optical constants of Sc show promising properties for filters or multilayers in the observed band, but further research is desirable both to fill the

spectral gaps that could not be covered in this research and to obtain in situ measurements in the whole spectral range.

The present optical constants were used to calculate the loss function $-\text{Im}(1/\varepsilon)$, with $\varepsilon = N^2$, for Sc films at wavelengths above 53.6 nm, which is shown in Fig. 5. The main feature of the figure is the peak centered between 92.0 and 96.4 nm (12.86-13.48 eV). A peak at 88.6 and ~89.2 nm (14.0 and ~13.9 eV) was obtained from EEL measurements by Brousseau-Lahaye et al.³ and Cukier et al.⁴, respectively. Brousseau-Lahaye et al.³ performed EEL measurements also for Sc hydride and oxide, which displayed peaks at 72.1 nm (17.2 eV) and 87.3 nm (14.2 eV), respectively. As mentioned in the introduction, the Sc metal samples measured in Refs. 3 and 4 had been apparently exposed to the atmosphere. Sigrist et al.² obtained the dielectric constant from Sc samples that were exposed to the air and found a peak that they reported to be centered at 95.3 nm (13 eV), even though the peak in Fig. 4 of Ref. 2 appears in fact centered at ~101.6 nm (12.2 eV). Sigrist et al.'s samples were oxidized, as they deduced from a broad peak of the loss function at 52.8 nm (23.5 eV). The present loss function data are then obtained first time from samples that were kept under UHV. The peak position seems to be independent of the sample being or not oxidized. The different peak positions found in the literature might be explained on the limited accuracy of the measurements, on the differences in sample preparation, and on sample reactivity under exposure to the environment.

Aging effects over the Sc film reflectance were measured. The near normal reflectance of a Sc sample, which will be referred to as sample 1, was measured soon after deposition, and after 3-day storage under UHV. The sample was then exposed to two

doses of air, which was allowed to flow into the chamber at a controlled pressure. The reflectance was measured after each dose. The first dose was given under a pressure of 10^{-1} Pa for a total exposure of 2×10^5 L (1 Langmuir $\equiv 10^{-6}$ torr x s, 1 torr = 133 Pa). The second dose was given under a pressure of 27 Pa for a total exposure of 2×10^7 L. Table 2 displays the reflectance decay. One more sample (sample 2) was characterized both freshly deposited and after a short storage period under UHV. The result is also displayed in Table 2. These data show that there is a reflectance decay under small doses of air and even under UHV. This reflectance decay on Sc is anyway smaller than the strong aging effects recently measured on Yb films¹⁹.

CONCLUSIONS

The optical properties of pure Sc films have been measured in the 6.7-174.4 nm spectral range. To our knowledge they have been measured for the first time within the whole spectral range. The optical constants n and k were obtained in the 53.6-174.4 nm range using in situ multi-angle reflectance measurements (106.7-174.4 nm) and multi-angle reflectance measurements along with transmittance measurements (53.6-104.8 nm). The extinction coefficient k was obtained at several wavelengths and bands within the 6.7-30 nm using ex situ transmittance measurements over C-Sc-C sandwiches. The extinction coefficient of Sc showed a peak at ~ 27 nm, whereas the Henke model predicts a peak centered at 32.7 nm. The current data show a strong disagreement with the Sc optical constants available in the literature, which were calculated using the Kramers-Kronig analysis starting with electron energy loss spectra on Sc samples that were apparently exposed to atmosphere. The difference was explained on the basis of the possible contamination of the latter samples. The loss function was calculated from the optical constants of pure Sc and it showed a peak centered at 92.0-96.4 nm. The position of the peak agrees within the experimental accuracy with previously published data obtained from electron energy loss spectra and from reflectance measurements on samples that had been exposed to the atmosphere.

The present research shows that Sc films have a low-absorption region in the ~ 27 -80 nm, assuming a smooth connection in the ranges that were not measured here, which makes Sc a promising candidate material for EUV filters and multilayers.

The aging of Sc films stored under UHV and later exposed to small doses of air under low pressure showed a decay in the EUV reflectance, which highlights the importance of measuring reflectance on samples deposited and maintained under UHV.

ACKNOWLEDGMENTS

We acknowledge Dr. Ermanno Jannitti (CNR, Padova) for his assistance in the organization of the research. José M. Sánchez Orejuela's technical assistance is gratefully acknowledged. We also acknowledge A. Iván Oliva (CINVESTAV, Mérida, Mexico) for measuring the roughness of glass substrates through AFM measurements. This work was partially supported by the National Programme for Space Research, Subdirección General de Proyectos de Investigación, Ministerio de Ciencia y Tecnología, project numbers ESP2001-4517-PE and ESP2002-01391. Partial support from the Italian Ministry of University and Scientific and Technological Research (MURST) through the COFIN Program is also acknowledged. Travel financial support was received from the CSIC-CNR joint programs.

References

1. J. H. Weaver and C. G. Olson, "Optical examination of the electronic structure of single-crystal hcp scandium", *Phys. Rev. B* **16**, 731-735 (1977).
2. M. Sigrist, C. Chassaing, J. C. François, F. Antonangeli, N. Zema, M. Piacentini, "Optical properties of scandium thin films", *Phys. Rev. B* **35**, 3760-3764 (1987).
3. B. Brousseau-Lahaye, C. Colliex, J. Frandon, M. Gasgnier, and P. Trebbia, "Determination of the electron excitation spectrum in scandium and yttrium by means of characteristic energy loss measurements", *Phys. Stat. Sol. (b)* **69**, 257-266 (1975).
4. M. Cukier, B. Gauthe, and C. Wehenkel, "Interband, collective and atomic (p, d) excitations from 2 to 160 eV in Sc, Y, lanthanides and actinides of their components by FEELS", *J. Physique* **41**, 603-613 (1980).
5. J. Onsgaard, S. Tougaard, P. Morgan, and F. Ryborg, "Scandium and lutetium surfaces studied by reflection electron energy-loss spectroscopy", *J. Electron Spectrosc. Relat. Phenom.*, **18**, 29-41 (1980).
6. Y. A. Uspenskii, S. V. Antonov, V. Yu, and A. V. Vinogradov, "Optical properties of 3d-transition metals in the spectral interval of interest for discharge pumped XUV lasers", in *Soft X-Ray Lasers and Applications II*, J. J. Rocca, L. B. Da Silva, eds., *Proc. SPIE* **3156**, 288-294 (1997).
7. Y. U. Uspenskii, V. E. Levashov, A. V. Vinogradov, A. I. Fedorenko, V. V. Kondratenko, Y. P. Pershin, E. N. Zubarev, V. Y. Fedotov, "High-reflectivity multilayer mirrors for a vacuum-ultraviolet interval of 35-50 nm", *Opt. Lett.* **23**, 771-773 (1998).
8. Y. U. Uspenskii, V. E. Levashov, A. V. Vinogradov, A. I. Fedorenko, V. V. Kondratenko, Y. P. Pershin, E. N. Zubarev, S. Mrowka, F. Schäfers, "Sc-Si normal incidence mirrors for a VUV interval of 35-50 nm", *Nucl. Instr. Meth. Phys. Res. A* **448**, 147-151 (2000).

9. J. A. Aznárez, J. I. Larruquert, and J. A. Méndez, "Far-ultraviolet absolute reflectometer for optical constant determination of ultrahigh vacuum prepared thin films", *Rev. Sci. Instrum.* **67**, 497-502 (1996).
10. Juan I. Larruquert, José A. Aznárez, José A. Méndez, "FUV reflectometer for in situ characterization of thin films deposited under UHV" in *Instrumentation for UV/ EUV Astronomy and Solar Missions*, Silvano Fineschi, Clarence M. Korendyke, Oswald H. Siegmund, and Bruce E. Woodgate, eds., *Proc. SPIE* **4139**, 92-101 (2000).
11. P. J. Goodhew, "Specimen preparation in materials science", Vol. I, Part I of the series *Practical methods in Electron Microscopy*, A. M. Glauert ed., North-Holland Publishing Company, Amsterdam, 1972; pp. 164-167.
12. A. M. Malvezzi and G. Secondi, "Calibration facility in the XUV Region for reflective optics", in *Ultraviolet and X-Ray Detection, Spectroscopy, and Polarimetry III*, S. Fineschi, B. E. Woodgate, R. A. Kimble, Eds, *Proc. of SPIE* **3764**, 40-48 (1999).
13. A. M. Malvezzi, G. Tondello, "A Grazing Incidence Spectrograph - Monochromator for XUV Spectroscopy in the 5 - 900 Å Region of Modular Concept", *Rev. Sci. Instrum.* **49**, 1642-1646 (1978)
14. D. H. Tombouliau, "The experimental methods of Soft X-Ray Spectroscopy and the Valence Band Spectra of the Light Elements" in *Handbuch der Physik*, Vol. XXX, Springer-Verlag, Berlin, 1957.
15. L. Poletto, A. Boscolo, G. Tondello, "Optical performances and characterization of an EUV and soft X-ray test facility", in *Ultraviolet and X-Ray Detection, Spectroscopy, and Polarimetry III*, S. Fineschi, B. E. Woodgate, R. A. Kimble, Eds, *Proc. of SPIE* **3764**, 94-102 (1999).

16. B.L. Henke, E.M. Gullikson, and J.C. Davis, "X-ray interactions: photoabsorption, scattering, transmission, and reflection at E=50-30000 eV, Z=1-92", Atomic Data and Nuclear Data Tables **54**, 181-342 (1993).
17. D.A. Attwood, "Soft X-Rays and Extreme Ultraviolet Radiation", Cambridge Univ. Press, Cambridge, 1999, p.91
18. http://www-cxro.lbl.gov/optical_constants/
19. J. I. Larruquert, J. A. Aznárez, J. A. Méndez, J. Calvo-Angós, "Optical properties of ytterbium in the far and the extreme ultraviolet", Appl. Opt. **42**, 4566-4572 (2003).

Table 1.a The extinction coefficient of Sc films at wavelengths shorter than 30 nm.

wavelength (nm)	k
6.7	0.0027±0.0004
9.2	0.0048±0.0005
11.4	0.0070±0.0005
13.5	0.0093±0.0006
17.30	0.0151±0.0007
17.67	0.0149±0.0004
18.06	0.0190±0.0005
18.23	0.0155±0.0006
18.61	0.0153±0.0005
19.00	0.0167±0.0008
19.58	0.0177±0.0008
19.97	0.0194±0.0016
20.33	0.0198±0.0013
20.89	0.024±0.003
21.32	0.023±0.003
21.51	0.023±0.003
24.67	0.102±0.002
24.74	0.100±0.002
25.00	0.090±0.002
25.30	0.111±0.003
25.74	0.126±0.005

26.17	0.144±0.004
26.52	0.184±0.014
26.78	0.169±0.020
27.23	0.194±0.005
27.68	0.176±0.005
28.14	0.162±0.007
28.59	0.154±0.005
29.06	0.134±0.004
29.52	0.134±0.003

Table 1.b The optical constants of Sc films at wavelengths longer than 50 nm.

wavelength (nm)	n	k
53.6	0.95±0.02	0.041±0.003
58.4	0.91±0.02	0.052±0.003
67.2	0.84±0.02	0.083±0.003
73.5	0.78±0.02	0.122±0.006
83.4	0.64±0.02	0.295±0.010
92.0	0.56±0.02	0.326±0.015
96.4	0.54±0.02	0.409±0.015
104.8	0.52±0.04	0.54±0.04
106.7	0.55±0.03	0.67±0.04
113.5	0.57±0.03	0.69±0.04
120.0	0.67±0.03	0.82±0.04
124.4	0.71±0.02	0.87±0.04
132.0	0.80±0.06	0.95±0.06
141.2	0.76±0.07	0.91±0.07
149.2	0.81±0.07	1.01±0.05
155.7	0.88±0.07	1.03±0.05
174.4	1.10±0.06	1.15±0.04

Table 2. Aging effects on the reflectance of Sc films that were stored 3 days in UHV and exposed to two doses of air at low pressure. The doses are expressed in Langmuirs.

λ (nm)	θ	Sample 1				Sample 2	
		Fresh	3 d UHV	2×10^5 L	2×10^7 L	Fresh	3 d UHV
104.8	5°	0.202	0.193	0.189	0.185		
120.0	5°	0.244	0.235	0.226	0.212		
58.4	5°					0.007	0.009
58.4	80°					0.582	0.547
104.8	5°					0.208	0.190
104.8	80°					0.800	0.796

Figure Captions

Fig. 1. The transmittance as a function of wavelength for Sc films of different thicknesses. The transmittance is normalized to that of the grid-supported C film substrate (in the 53.5-174.4 nm wavelength range), and to that of a reference C-C-grid sample (in the 6.7-30 nm wavelength range)

Fig. 2. The reflectance of Sc films versus wavelength at nine angles of incidence measured from the normal in the horizontal plane of incidence of the reflectometer.

Fig. 3. The logarithm of the transmittance versus Sc film thickness for several wavelengths and the fitting with Eq. 1. Transmittance was measured for Sc films deposited over a C film supported on a grid. Measurements at 9.2 and 13.5 nm were performed on samples that had a passivating top C layer also.

Fig. 4. The logarithm of the optical constants of Sc as a function of wavelength in the 53.6-174.4 nm (a) and 6.7-30 nm (b). Calculations with Henke model and the optical constants data from Brousseau-Lahaye et al.³ are shown for comparison.

Fig. 5. The loss function of Sc as a function of wavelength.

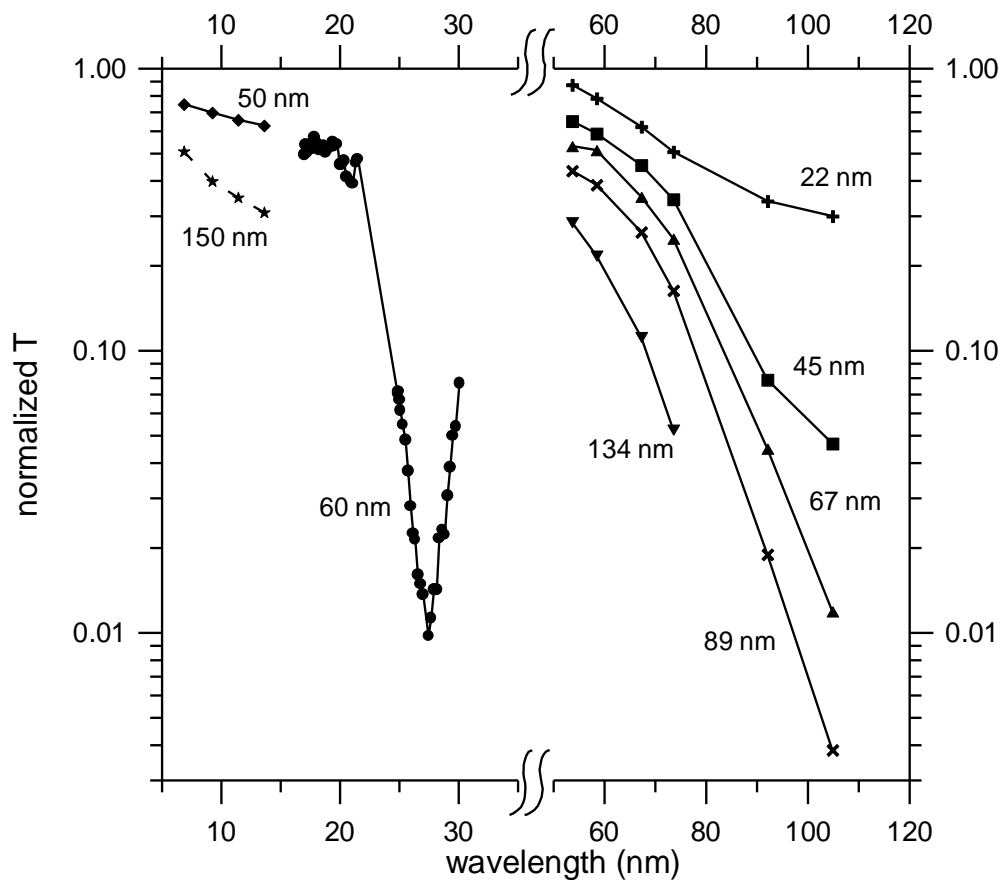


Fig. 1.
 Juan I. Larruquert
 Applied Optics

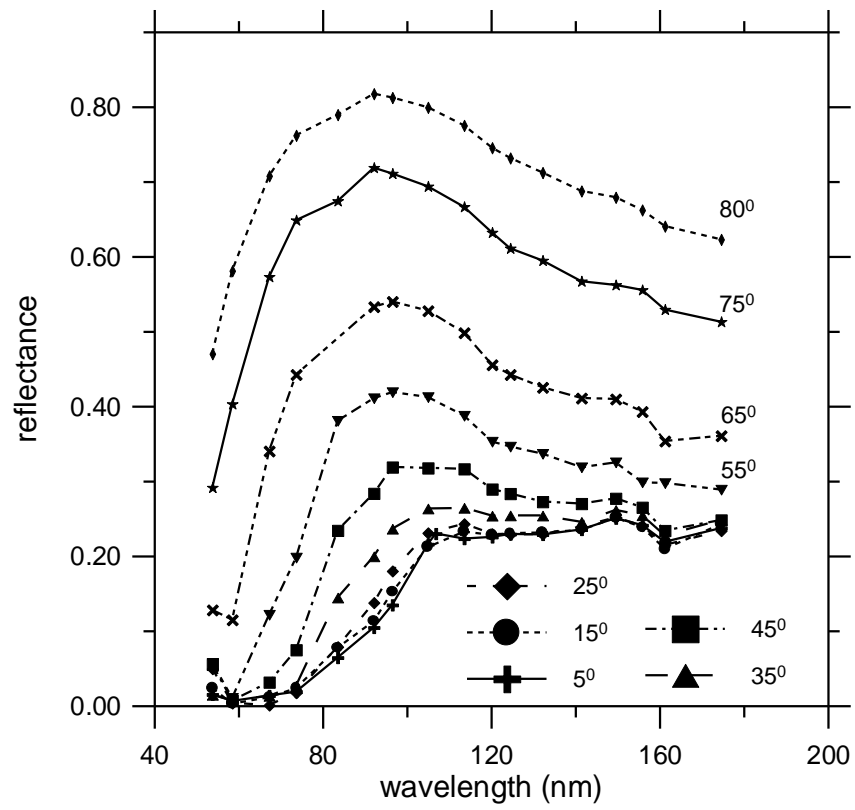


Fig. 2
 Juan I. Larruquert
 Applied Optics

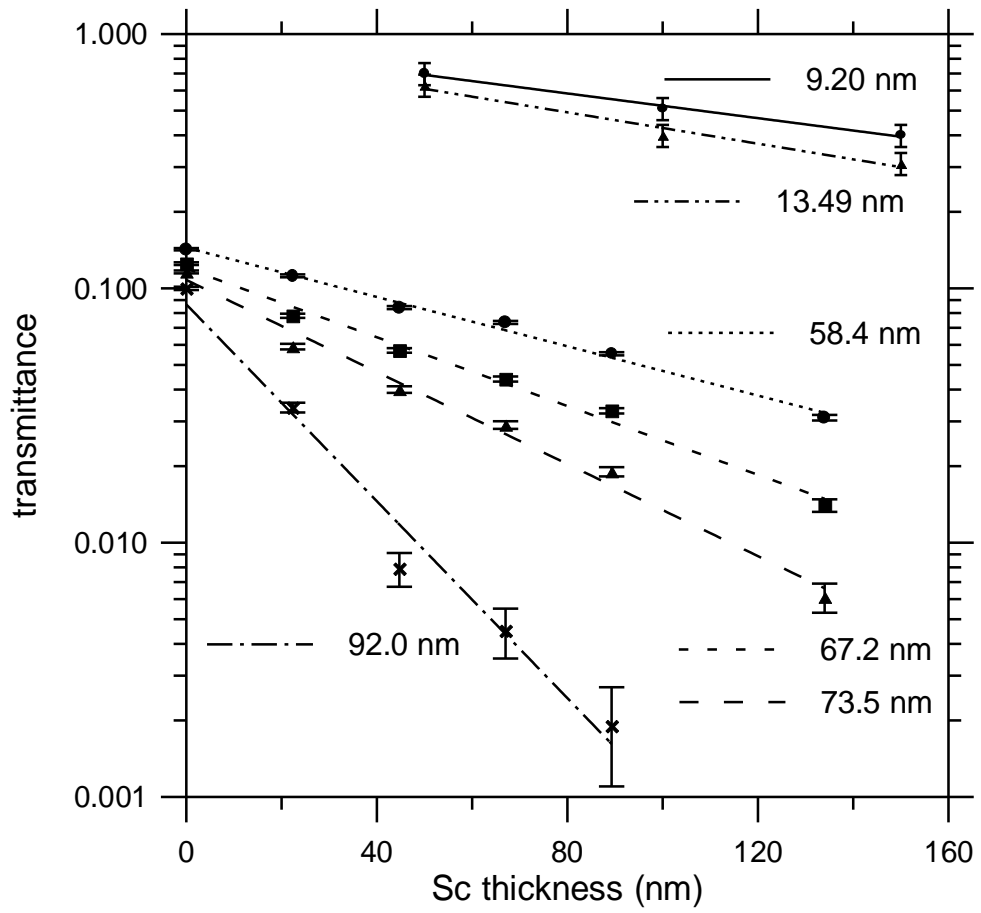


Fig. 3.
 Juan I. Larruquert
 Applied Optics

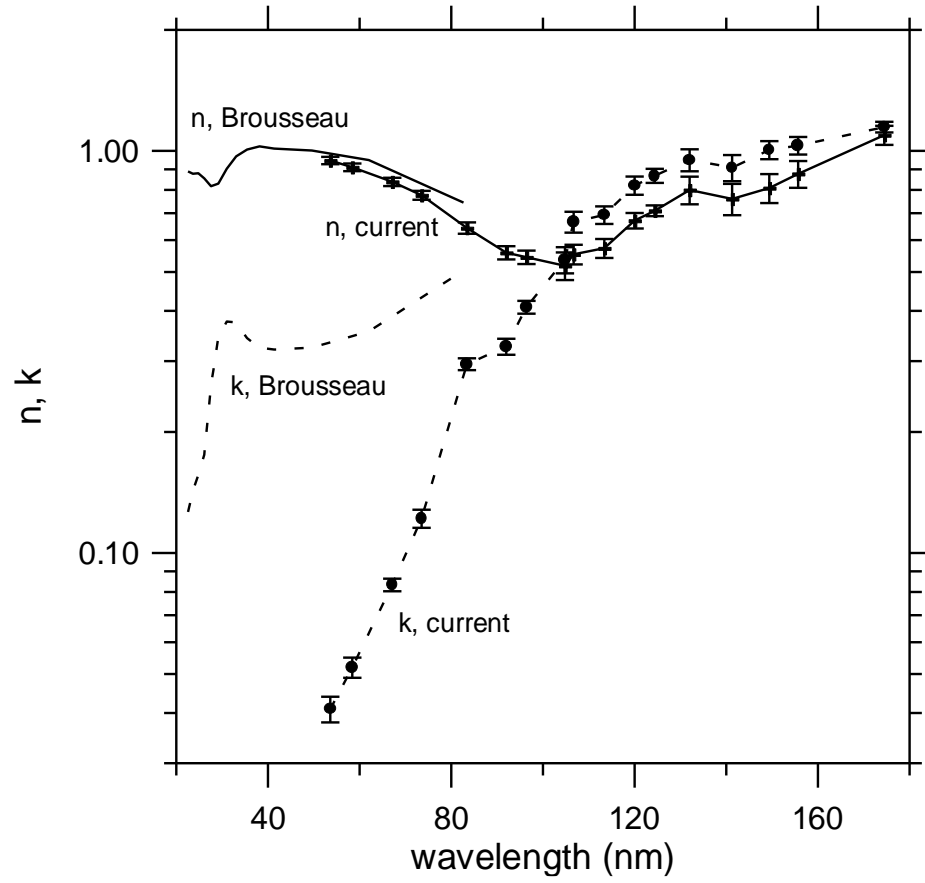


Fig. 4a.
Juan I. Larruquert
Applied Optics

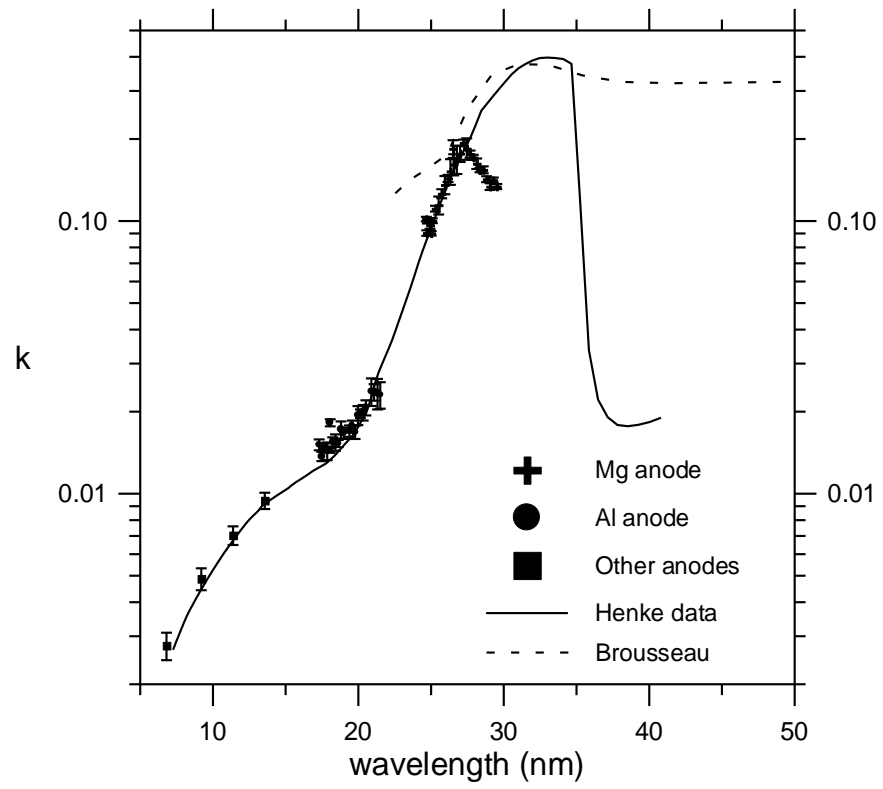


Fig. 4b
Juan I. Larruquert
Applied Optics

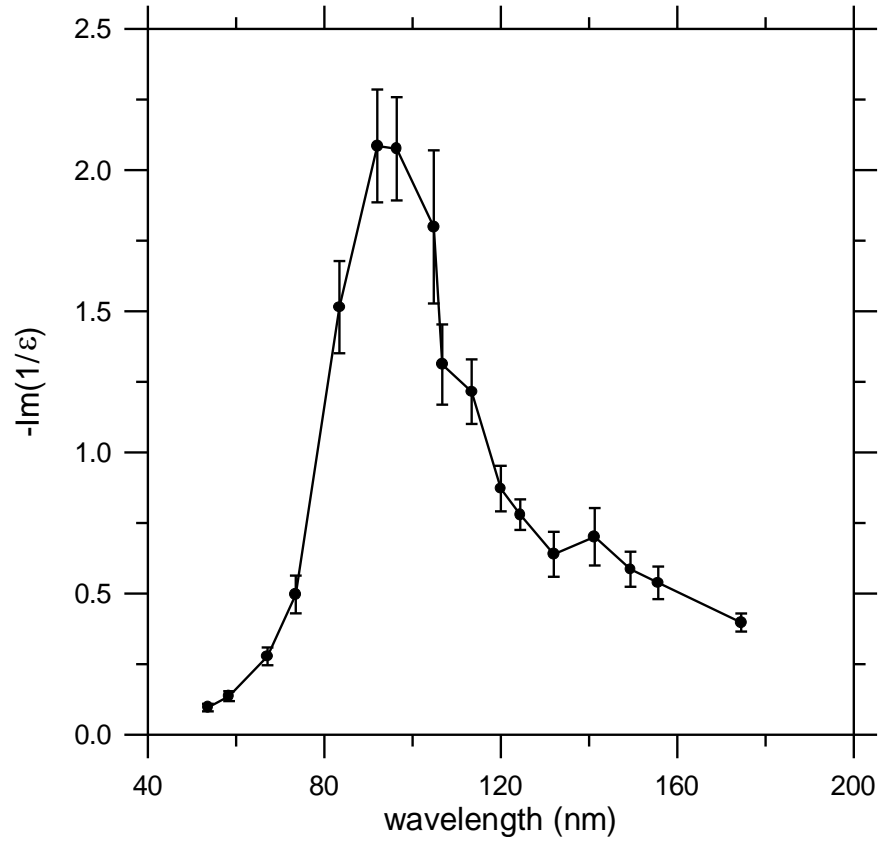


Fig. 5
Juan I. Larruquert
Applied Optics